Numerical Simulation of Aerofoil with Flow Injection at the Upper Surface

Open Access

Chua Bing Liang[1], Akmal Nizam Mohammed[1,*], Azwan Sapit[1], Mohd Azahari Razali[1], Mohd Faisal Hushim[2], Amir Khalid[2], Nurul Farhana Mohd Yusof[3]

[1] Faculty of Mechanical and Manufacturing Engineering, Universiti Tun Hussein Onn Malaysia, 86400, Parit Raja, Batu Pahat, Johor, Malaysia
[2] Faculty of Engineering Technology, Universiti Tun Hussein Onn Malaysia, Pagoh Higher Education Hub, 84600 Pagoh, Muar, Johor, Malaysia
[3] School of Mechanical Engineering, Engineering Campus, Universiti Sains Malaysia, 14300 Nibong Tebal, Pulau Pinang, Malaysia

ARTICLE INFO	ABSTRACT
	Separation of the boundary layer over an airfoil causes a significant increase in the adverse pressure gradients and the losses of energy resulting in the reduction of the lift force and the increment of drag force. Therefore, delaying and eliminating flow separation is necessary to improve its aerodynamic characteristics. In this study, an injection of flow was introduced at the upper surface/suction side of the aerofoil to control the boundary layer separation effectively. Flow around the NACA0012 airfoil was examined, with the position of flow injection jet at 90° relative to the tangential surface of the airfoil at 20%, 50% and 80% of its chord length. The flow injection velocity was varied from 0%, 10%, 30% and 50% of the free stream velocity, which corresponds to 0, 2.5 x 10-4, 2.25 x 10-3 and 6.25 x 10-3 of the momentum coefficient. The results showed that the most suitable condition was at 10% of the blowing amplitude (2.5 x 10-4 of the momentum coefficient) of flow injection at the trailing edge, which was around 80% of the chord length at the upper surface/suction side. This configuration can successfully increase the lift force and decrease the drag force of the aerofoil at the angle equal to or larger than a stall angle of 16° compared to the baseline aerofoil.

1. Introduction

The airfoil is the main reason why an aircraft can take flight. Airfoils are thin, streamlined bodies that allow smooth passage of air around its profile by splitting flow to its upper and lower surfaces. They are a major determinant of cruising speeds, stall speed, take-off and landing distances, as well as the overall aerodynamic characteristics of an aircraft [1]. The wing's upper surface is shaped (curved) to accelerate the air and decrease the pressure at the top, while the airspeed and pressure at the bottom along the flatter lower surface remain comparatively unchanged. This results in a pressure difference between the upper and lower surfaces, producing lift. However, the creation of lift also induces a drag force that acts in the opposite direction of the flow [2, 20]. The drag

---

component is highly related to the flow phenomenon commonly known as flow boundary layer separation.

Boundary layer separation control is very important for the performance and the maneuverability of the airplanes. Thus, it is crucial to incorporate the effective boundary layer mechanism. In previous studies, aerodynamic characteristics of the airfoil were enhanced by changing the blade profile. For example, Mahmud *et al.,* [3] studied bi-camber surfaces in airfoils which are surface profiles that have two or more raised ridges placed laterally to fluid flow, running parallel to the leading and trailing edge. He proved that the lesser vortex effect in the bi-camber profile results in the increment of the lift to drag ratio of the airfoil. Jain *et al.,* [4] studied the gurney flap, a micro tab fitted at the trailing edge of the airfoil on its pressure side to increase the lifting force of the airfoil. There are also many techniques and control methods to delay and eliminate the boundary layer separation effectively such as the passive flow control and the active flow control methods [5, 6].

Passive flow control is a method that manipulates geometrical effects by incorporating additional attachments such as the vortex generator and providing the surface roughness also known as dimples. Separation control is achieved by controlling the pressure gradient in this method. The disadvantage of using this method is that the massive drawback with the pressure flow control will increase the profile losses, which cannot be deactivated when it is not required [7]. Lee *et al.,* [8] studied the vortex generator which is the rectangular or triangular attachments with the height almost equal to the boundary layer thickness positioned obliquely to create the energetic vortices and leads to the boundary layer mixing enhancement. Alternatively, dimples can emulate surface roughness providing the method to create vortices, resulting in the turbulence effect that helps to delay the boundary layer separation to increase the stall angle, decrease the drag and stabilize the aircraft during a stall.

On the other hand, the active flow control is a method that introduces momentum into the boundary layer and increases the energy so that the boundary layer can keep attached to the profile, delaying the flow separation. Active flow control can be divided into two which are additional mass injection control and without additional mass injection control method [7]. Additional mass injection control introduces continuous blowing or suction at the upper surface of the airfoil. Huang *et al.,* [9] and Prakash *et al.,* [10] had studied the effect of the continuous blowing and suction at the upper surface of the airfoil and the results show that the steady suction perform better than the steady blowing as the suction can create a lower pressure and increase the lifting effect at the upper surface of the airfoil. The amount of secondary fluid needed in the continuous flow injection is increased and thus the pulsed blowing method is introduced and studied by Deng *et al.,* [11] and De Giorgi *et al.,* [12]. They have proved that the pulsed blowing will not reduce the performance as the additional mass injection control, instead it performs better than the continuous blowing method. However, this kind of method is less effective than the method without additional mass injection control from the viewpoint of regaining energy.

The method of active flow control without additional mass injection is also known as the zero net mass flux jet control. Examples of this include the synthetic jet and the co-flow jet, CFJ. You *et al.,* [13] and Zhao *et al.,* [14] showed a practical use of the synthetic jet, a piezoelectric diaphragm that is used to drive one side of the cavity in a periodic manner where the flow can go into the cavity and could be evacuated. This setup can promote the mixing of the boundary layer by adding or removing the momentum to or from the boundary layer with the formation of the vortical structures. The co-flow jet is the control that introduces an injection slot near the leading edge and a suction slot near the trailing edge at the upper surface of the airfoil. Additionally, Lefebvre *et al.,* [15] and Abinav *et al.,* [16] had studied the CFJ in delaying and eliminating the boundary layer separation and show that

the injection and suction of the CFJ can synergize and enhance the boundary layer momentum and the airfoil circulation.

In the present study, simulations are performed to analyze and compare the effect of applied perpendicular blowing control on NACA0012 airfoil with baseline airfoil and to determine the optimum perpendicular blowing condition for enhancing the aerodynamic characteristics of the airfoil, which corresponds to the lower drag, higher lift and lift to drag ratio. As opposed to previous studies involving passive and active flow control mentioned, this study aims to observe the effects of blowing at higher angles of attack nearing stall. This is so that the lift coefficient of the airfoil is increased at these higher angles, and possibly delay stall itself.

2. Methodology

The ANSYS CFX software was used to perform all simulations and analysis. Standard settings are used in creating the structure of the airfoil, the meshing process, the boundary condition setup, and the solver controls unless stated otherwise. After getting the analysis and simulation result by ANSYS CFX, validation with the experimental data available in literature was done in order to verify the accuracy and the validity of the results.

2.1 Parameter Selection

The parameters related to the NACA0012 airfoil is described in Table 1.

Table 1
Parameters of the aerofoil

Parameter	Details
Type of aerofoil	NACA0012
Chord length	1 m
Angle of attack	0°, 10°, 16°, 18°

The angles of attack chosen represent conditions of zero lift, medium-lift, high lift, and near stall respectively. To find the inlet free stream velocity (U), the standard Reynolds number was used [19]:

$$Re = \frac{\rho U L}{\mu} \tag{1}$$

Here, Re is Reynolds number, ρ is density, U is velocity, L is the length, μ is dynamic viscosity and υ is kinematic viscosity. To relate with the study case, length (L) is substituted with the chord length of the airfoil. Table 2 shows the parameter of the fluid flow over the airfoil.

Table 2
Parameters of flow

Parameter	Details
Reynolds number	1.00×10^6
Free stream velocity	15.62 m/s
Temperature	25 °C
Atmospheric pressure	1 atm
Density	1.18 kg/m^3
Dynamic viscosity	1.85×10^{-5} kg/m.s
Kinematic viscosity	1.56×10^{-5} m^2/s

To find the jet entrance velocity as set in Ref. [9], the following equations were used:

$$U = A\cos(\theta\beta) \text{ in the x-direction} \tag{2}$$

$$V = A\sin(\theta\beta) \text{ in the y-direction} \tag{3}$$

Relating to the study, β is the angle between the free stream velocity direction and the local jet surface, and θ is the angle between the local jet surface and the jet entrance velocity direction. The blowing amplitude of the flow injection also can be expressed in another term, which is the jet momentum coefficient, C_μ, which is obtained by Huang *et al.,* [9]:

$$C_\mu = \frac{\rho \cdot h \cdot \sin(\theta)V^2}{\rho \cdot C \cdot U^2} = \frac{h}{C}A^2, \text{ where } A = \frac{V}{U} \tag{4}$$

Other parameters related to the injection of flow are shown in Table 3. Each simulation case utilize a combination of each parameter value.

Table 3
Parameters of the injection

Parameter	Details
Type of injection	Steady blowing
Width of injection slot	2.5% of the chord length
Position of injection slot	40%, 60% and 80% of the chord length
Blowing ratio	10% and 20% of the freestream velocity
Momentum coefficient	0.0×10^0, 2.5×10^{-4} and 1×10^{-3}

2.2 Computational Domain and Grid Setup

The grid studies of the airfoil are two-dimensional multi-zonal blocks. The dimension of the wide region of the computational area is chosen as 14C of width times 21C of length in order to prevent the outer boundary form affecting the flow field around the airfoil. The cell size for the wide region was set as 0.1m while for the influencing region; the size of the cell was set as 0.02 m. For the second inlet portion, the smaller size of the grid was set so that the more accurate simulation result can be obtained.

The number of grids of the airfoil blocks and the background blocks is critical. Hence, four different numbers of grid densities were conducted in order to obtain a more accurate result that approaching the answer. 100 iterations and 1×10^{-6} RMS was set as the convergence criterion to get the best converge solution with the desired accuracy set by the users. The meshing also must reach the acceptable skewness so that the solution can be converged.

For the outlet and ambient boundaries, the condition was set as opening and the 0 atm is set as the relative pressure. The far fields were given the velocity boundary condition of 15.62 m/s along the x-direction according to 1 million of the Reynolds number while the applied perpendicular injection was given the inlet velocity boundary condition perpendicular normal to the wall. Figure 1 shows the wide region and the influencing region around the airfoil.
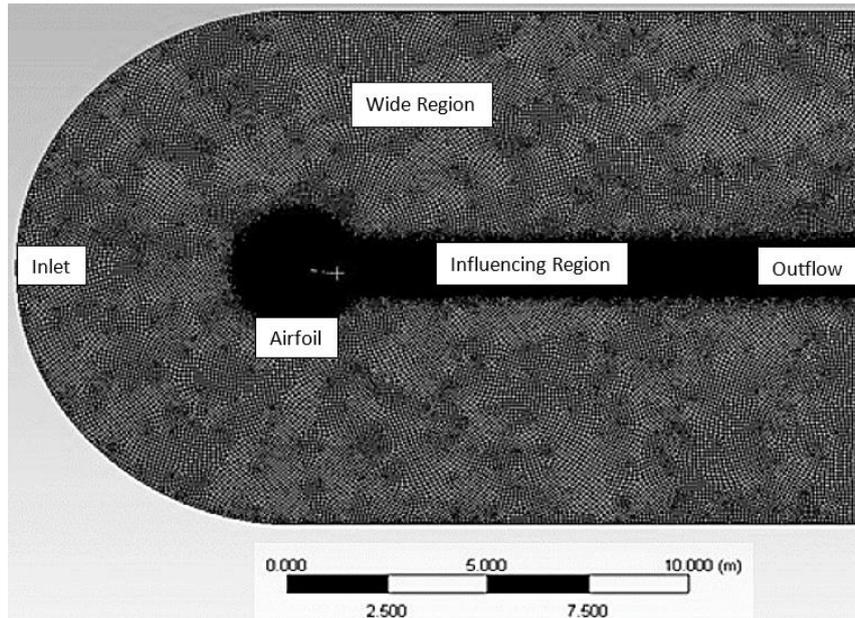
Fig. 1. The wide region and the influencing region of the airfoil

3. Results

The discussion is mainly focused on the pressure coefficient, C_P, lift coefficient, C_L and drag coefficient, C_D of the different angles of attack, AoA and compare the results of baseline airfoil and the airfoil with the applied blowing control.

3.1 Grid Independence

In order to find the more suitable number of nodes to be used in the meshing process, the grid independence test of C_L & C_D of the baseline NACA0102 aerofoil of the Reynolds number equals 1 million with the 4 different number of nodes is carried out. The simulation is continued until the lift and drag coefficients fully converged. Figure 2 shows the graph of the grid independence test and Table 4 shows the CL & CD of Different Number of Nodes at AOA of 16°.

From Figure 2 and Table 4, the results of C_L and C_D did not vary significantly with regards to the node count. Thus, the mesh configuration adopted for all subsequent work has 225,816 nodes.
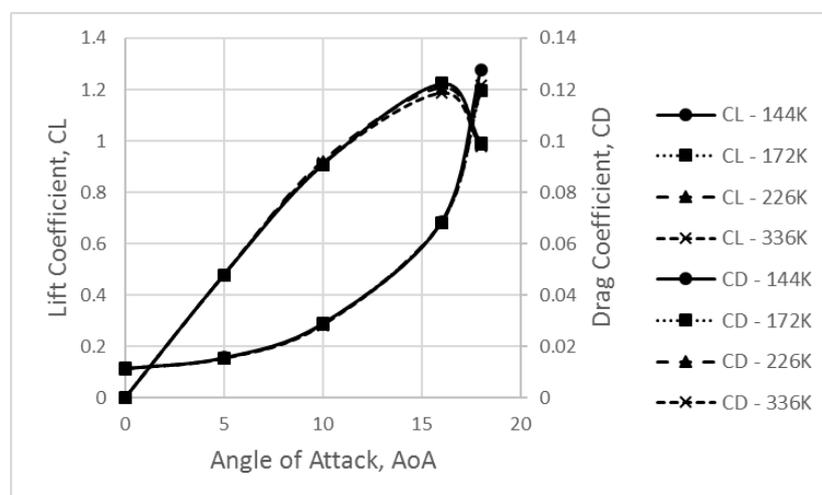
Fig. 2. Grid independence results of the baseline airfoil

Table 4
C_L & C_D of baseline aerofoil at AoA of 16°

Number of nodes	Lift Coefficient, C_L	Drag Coefficient, C_D
1.44×10^5	1.22	0.068
1.72×10^5	1.22	0.068
2.26×10^5	1.21	0.067
3.36×10^5	1.19	0.068

3.2 Validation of NACA0012 Aerofoil

For validation, the result of the baseline aerofoil simulation for the present study is compared with the simulation result by Huang *et al.,* [9] and the theoretical result of Airfoil Tools and shown in Figure 3. In Figure 3, it can be seen that most of the theoretical calculation result is higher than the simulation results. The difference between the theoretical calculation and simulation result can be due to only 2D analysis is conducted. This is because there is a limitation for the planar dimensional analysis. For example, the three-dimensional vorticity which is very significant in the separation of the boundary layer is not considered in the simulation. There is only a small difference between the simulation result by Huang and the present study. This may be due to the selection of the turbulence models, artificial viscosity and the grid density that causes the difference between the simulation results [7, 9].

According to the previous study, the researchers had proposed many values of stall angle of NACA0012 airfoils such as 10° and 14°. This is due to the selection of turbulence model selection that significantly influences the changes of the stall angle [7, 17]. The previous researchers also had proved that Menter's shear stress transport turbulence model (SST) always gives better results than the K-epsilon two-equation model. K-epsilon's realizable model is quite good in the prediction of the pre-stall region but it cannot predict well at both the stall and post-stall conditions. The results of previous studies showed that for the lower Reynolds number, the SST turbulence model gives the more reliable results while for the higher Reynolds number, the K-epsilon model is more suitable [17].

From the Figure 3, it is observed that there is a much difference in the results at the angle of attack of 16°. The maximum relative error between the present study and the theoretical calculation is about 22% for C_L and 91% for C_D. However, there is only 13% for C_L and 77% for the C_D of the average percentage of relative error. While for the maximum relative error of the simulation result by Huang *et al.,* [9] and the present study is only 7% for C_L and 43% for C_D. However, the average percentage of relative error is just 2% for the C_L and 30% for the C_D.
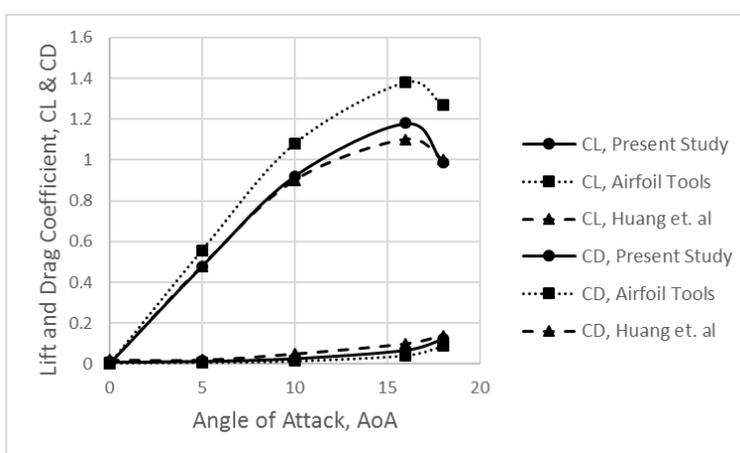
Fig. 3. Validation result of C_L and C_D for the baseline airfoil

3.3 Simulation Results for Different Blowing Conditions

The comparison between the C_L and C_D of different blowing location of 20%, 50% and 80% of airfoil chord length and amplitude of 10%, 30% and 50% of free stream velocity (momentum coefficient of 2.25 x 10^{-4}, 2.25 x 10^{-3} & 6.25 x 10^{-3}) are shown in the Figure 4, Figure 5 and Figure 6.

Generally, all the graphs show that as the AOA increases, the value of C_L and C_D also increases but the increasing rate of C_D is very small compared to the C_L until it reached the 16°, which is the stall angle and further increasing of AOA will cause the C_L decreases rapidly and C_D increases significantly. Besides that, from the overall results, it also can be seen that for the blowing amplitude, A=0.1 (momentum coefficient of 2.5 x 10^{-4}) of all the blowing locations at the various angles of the attack had recorded a higher values of C_L and a lower values of C_D as compared with the other blowing amplitudes. This shows that the optimum blowing amplitude is 10% of the free stream velocity, which corresponds to 2.5 x 10^{-4} of the momentum coefficient.

Other than that, it also can be observed that, for the blowing location at 80% of the airfoil chord length with the blowing amplitude of 0.1 (momentum coefficient of 2.5 x 10^{-4}), this setting recorded the highest value of C_L and the lowest value of C_D at stall angle of 16°. In comparison, other blowing locations of 20% and 50% of the airfoil chord length resulted in lower C_L and higher C_D. Hence, it can be concluded that the most suitable condition for the better blowing control is at the location of 80% of the airfoil chord length, 80% C with the blowing amplitude of 10% of the free stream velocity, A=0.1 (momentum coefficient of 2.5 x 10^{-4}).
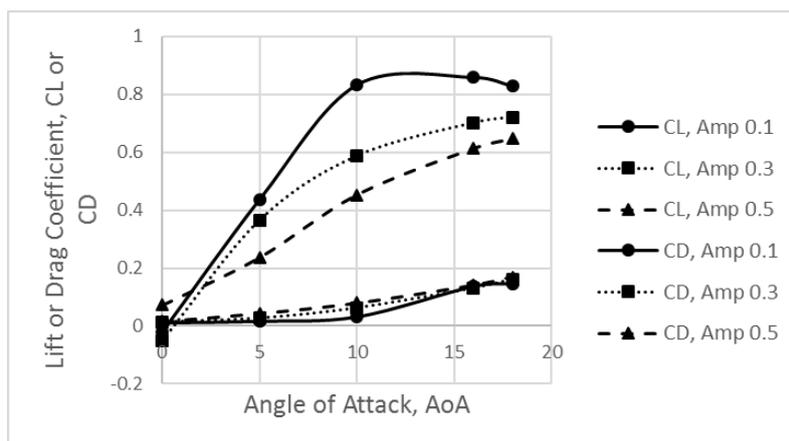
Fig. 4. C_L and C_D for different blowing amplitudes at L_J/C = 20% C
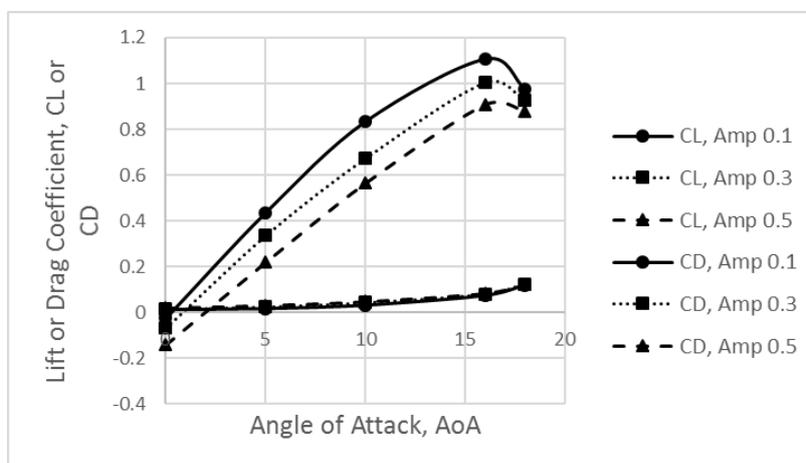
Fig. 5. C_L and C_D for different blowing amplitudes at L_J/C = 50% C
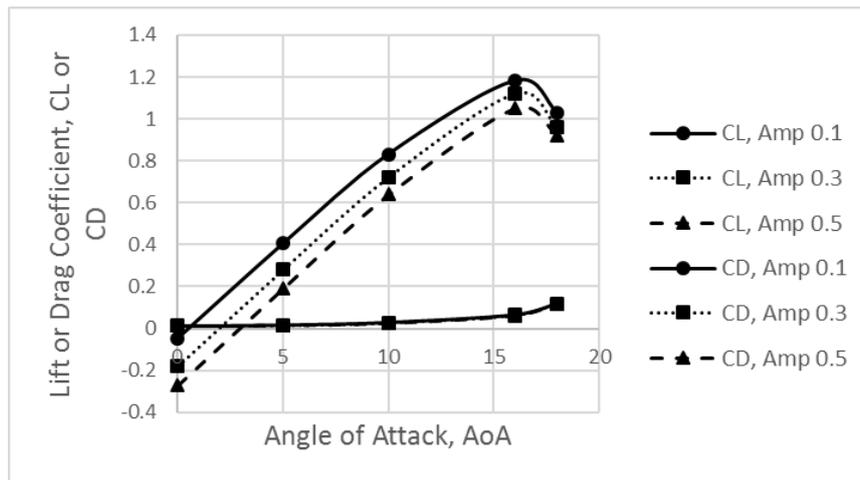
Fig. 6. C_L and C_D for different blowing amplitudes at L_J/C = 80% C

3.4 Effectiveness of Boundary Layer Control

To determine the effectiveness of the boundary layer control of different blowing location, the comparison between the graphs and table of C_L, C_D and lift to drag ratio at different blowing location of 0.1 blowing amplitude, which corresponds to the momentum coefficient of 2.5 x 10^{-4} with the baseline case (no blowing) is shown in Figure 7 and Figure 8.

From Figure 7 and Figure 8, most of the applied blowing controls show an undesirable result which is a lower value of C_L and lift-to-drag ratio and higher values of C_D as compared with the baseline case. However, it is also observed that the conditions had improved (C_L and lift to drag ratio increase, C_D decreases) when the blowing control is applied at the locations that approaching the trailing edge which is 50% C and 80% C. This prove that the trailing edge blowing is better than the leading edge blowing. At the optimum blowing location of 80% C, starting from the angles of attack equal and larger than the stall angle which is 16° and 18°, the results had recorded a higher value of C_L and a lower value of C_D and resulting to a higher lift to drag ratio as compared to the baseline case.
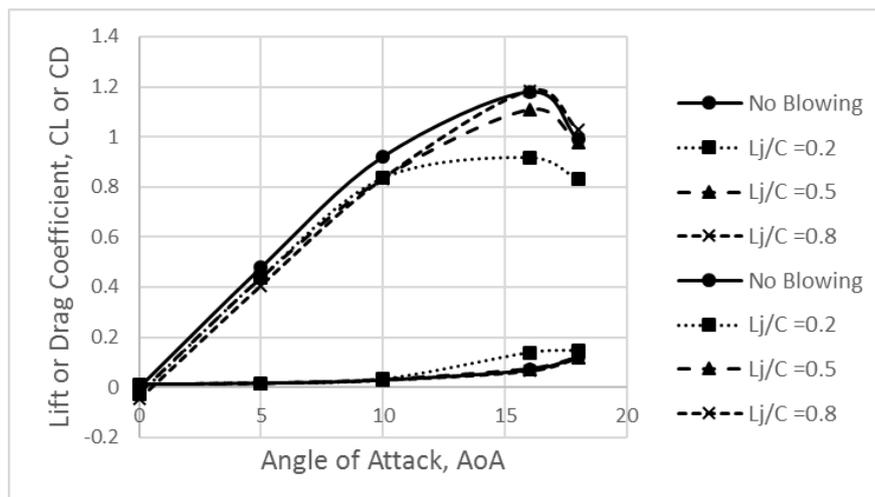
Fig. 7. C_L and C_D vs. AoA at different blowing locations, with blowing amplitude of 0.1
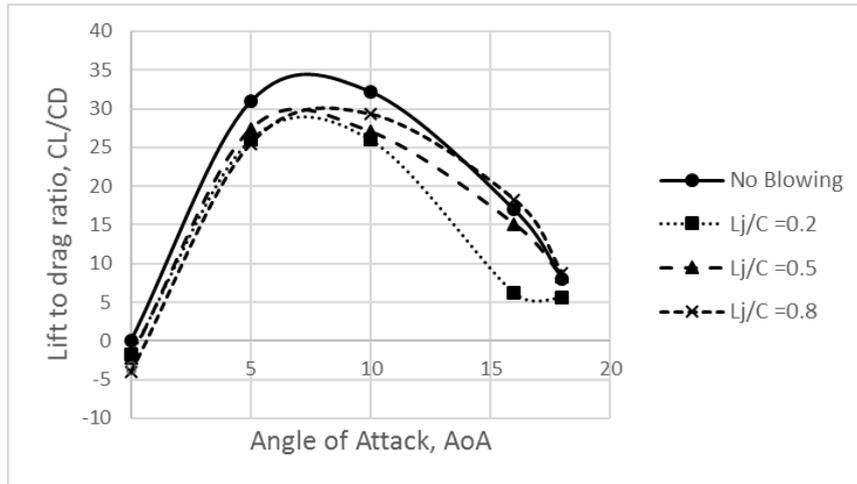
Fig. 8. Lift to drag ratio vs. AoA at different blowing locations, with blowing amplitude of 0.1

Figure 9 and Figure 10 show a better boundary layer control is achieved at the angles larger or equal to the stall angle which is 16º and 18º (C_L & lift to drag ratio increase, C_D decreases) when the blowing amplitude is small as compared to the baseline case. This can be proved when the blowing amplitude is 0.1 (momentum coefficient of 2.5 x 10^{-4}), C_L & lift to drag ratio is increased and C_D is decreased as compared to the baseline case. When the blowing amplitude is 0.3 (momentum coefficient of 2.25 x 10^{-3}), the graph of lift to drag ratio vs AOA had recorded a higher value compared to the baseline case although the value of C_L is lower than the baseline case. This is due to the lower value of C_D as compared to the baseline case.

When the blowing amplitude is sufficiently high, the condition becomes worse than the baseline case. This can be seen when the blowing amplitude is 0.5 (momentum coefficient of 6.25 x 10^{-3}), the results had recorded a lower value of C_L and lift to drag ratio, a higher value of C_D compared to the baseline case. Hence, it can be concluded that the suitable blowing condition is when A=0.1 which corresponds to 2.5 x 10^{-4} of the momentum coefficient.
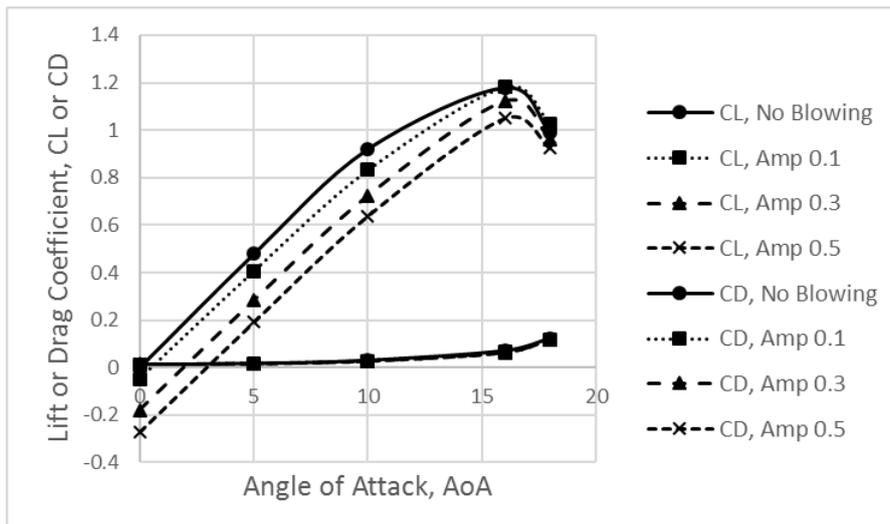
Fig. 9. C_L and C_D vs. AoA for different blowing amplitudes at blowing location of 0.8C
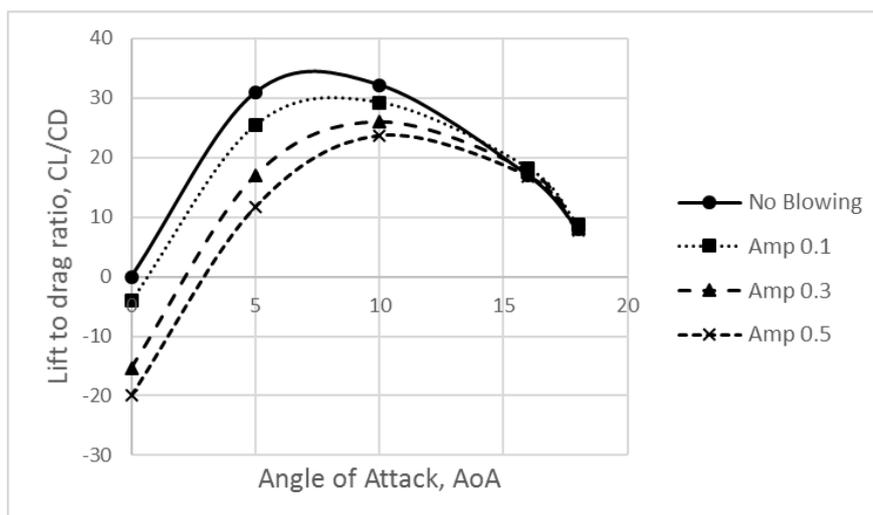
Fig. 10. Lift to drag ratio vs. AoA for different blowing amplitudes at blowing location of 0.8C

In order to determine the efficiency of the better boundary layer control, the comparison of the percentage increase or decrease of the lift to drag ratio had been made between optimum blowing condition of 0.8 C blowing location and blowing amplitude of 0.1 (2.5×10^{-4} of the momentum coefficient) with the baseline case and is recorded in Table 5. Here, it can be seen that at the angle of attack of 16°, the value of C_L increases from 1.17988 to 1.18207, the value of C_D decreases from 0.06961 to 0.06480 and a total of 7.08% increase of the lift to drag ratio. While at the angle of attack of 18°, the value of C_L increases from 0.98950 to 1.02741, the value of C_D decreases from 0.12261 to 0.11736 and a total 8.48% increase of the lift to drag ratio.

Therefore, this had proved that a better boundary layer control is achieved at the optimum condition of blowing amplitude of 0.1 (2.5×10^{-4} of momentum coefficient) and the blowing location of 0.8 C.

Table 5
The values of Reynolds number and velocity

AoA	C_L/C_D (No Blowing)	C_L/C_D (L/C = 0.8)	% C_L/C_D Increase
0	0	-4.08	–
5	30.95	25.43	-17.83
10	32.21	29.26	-9.16
16	16.95	18.24	7.08
18	8.07	8.75	8.48

3.5 Analysis of Pressure Coefficients

Streamline will show the curves that are instantaneously tangent to the velocity vector of the flow. The pressure coefficient C_P is a dimensionless number that describes the relative pressures throughout a flow field in fluid dynamics while the closed area within the C_P curve indicates the amount of lift [18, 9]. The graph of pressure coefficient C_P between different blowing amplitude of $L_j/C=0.8$ C at AOA of 18° is shown in Figure 11. It can be seen in Figure 11 that the closed area within the C_P curve of blowing amplitude of 0.1 is the largest which means the lift is the largest among the other case [9]. As the blowing amplitude increases, the vortex formed at the downstream also increases which increases vortex circulation decreases the downstream upper surface C_P and

increases the lift. On the contrary, the upper surface C_P and shear stress due to the direct effect of blowing near the vicinity of the jet will be increased and thereby increases the skin-friction drag and decreasing the lift. The net effects of these driving factors contribute to the increase of drag and decreasing lift [9].

When the blowing amplitude increase to 0.3, it is observed that the blowing control causes the obstruction to the main streamflow. The larger vortex formed are not able to exchange the momentum with the mainstream and thus yield a higher drag and lower lift [7]. When the blowing amplitude increased to 0.5, the increase blowing velocity causes a massive obstruction that the mainstream is not able to flow along with the applied blowing control. This will result in a rapidly decreasing lift which corresponds to the smallest closed area within the C_P curve in Figure 11.

Hence, it can be concluded that the higher amplitude of blowing will create a disturbance that prevents the flow from reattaching efficiently.
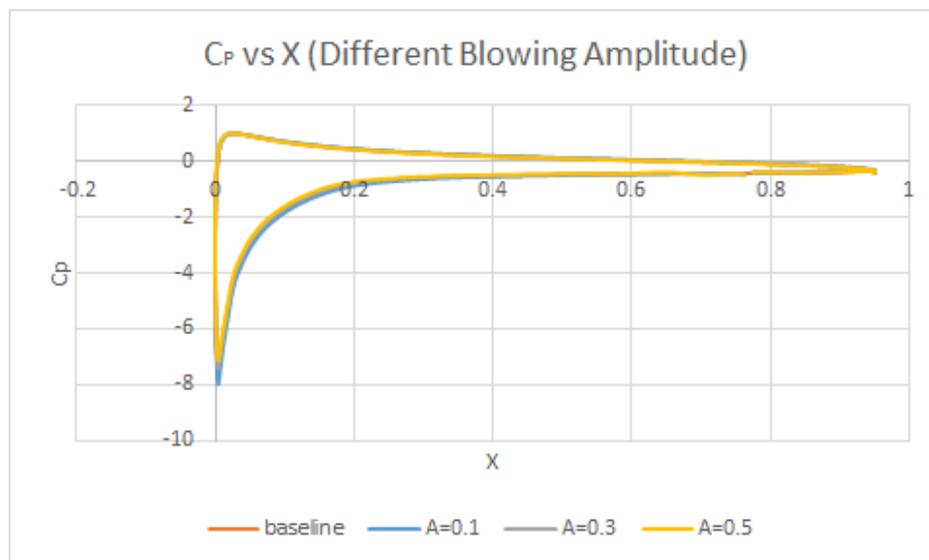
Fig. 11. C_P vs. airfoil location for different blowing amplitudes

The graph of pressure coefficient, C_P between different blowing location of 0.1 blowing amplitude at AOA of 18° are shown in Figure 12. Here, the value of C_P with the blowing location of 20% C increases rapidly to the highest value among the other cases and although the value after the jet decreases, the end results to yield the smallest closed area within the C_P curve and this corresponds to the lowest lift compared to the other cases [9]. When the location of the perpendicular blowing control moves downstream to the locations of 50% C, the vortices formed are smaller and more suppressed which corresponds to the increased of the closed area within the C_P curve compared to the leading edge blowing but the result is still worse than the baseline case [9].

Only at the blowing locations of 80% C does the boundary layer control have a positive effect in enhancing the aerodynamic characteristics of the airfoil. This can be seen in Figure 12 where the vortices formed is the smallest and the closed area within the C_P curve is the largest among the other cases. This is because the blowing slot is located close to the separation point as proposed by Zheng *et al.,* [7] who started the better boundary layer control can be achieved when the secondary blowing slot is located close to the separation point. As the boundary layer thickness is less at the beginning of the separation point, this will reduce the required momentum for the mixing initiation.
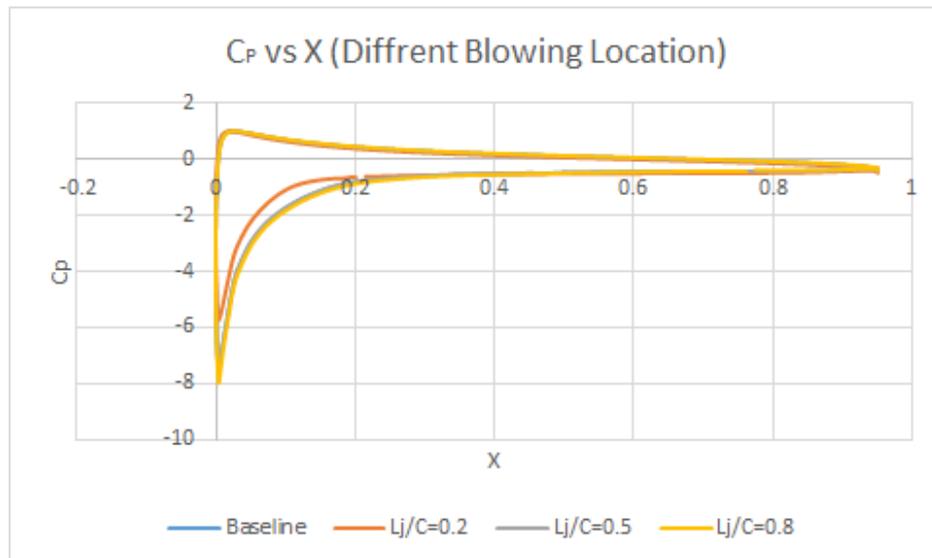
Fig. 12. C_P vs. airfoil location for different blowing locations

4. Conclusions

In conclusion, the present study shows a good agreement with the simulation result of the previous study and the theoretical calculation. Through this study, the effects of steady perpendicular blowing on NACA0012 aerofoil on the separation control are analyzed and the following results are gained.

First, the steady perpendicular blowing causes the larger vortices and makes most of the situations worse than the baseline case. Steady perpendicular blowing with the conditions of blowing amplitude of 0.1 (2.5×10^{-4} of the momentum coefficient) and the locations of 80% C is useful for the angles of attack equal or larger than the stall angle while it has no favorable effects on the aerodynamic characteristics at the angles of attack that are smaller than the stall angle. This suitable condition of blowing is able to enhance the aerodynamic characteristics by successfully reducing the drag, increasing the lift and the results of a total of 7% to 8%, an increment of the lift to drag ratio is obtained.

Besides that, for the steady perpendicular blowing location perspective, the closer the applied perpendicular blowing slot location to the natural separation point of the aerofoil, the more favourable of the effects of the aerodynamic characteristics. Leading-edge blowing generates the larger vortices and greater circulation about the aerofoil that can increase the lift but at a cost significantly increases the pressure at the leading edge and causing the detachment of the flow. Thus, the net effect increases the pressure drag and decreases the lift. On the other hand, downstream blowing can improve the lift and reduce the drag but smaller amplitude is better than higher amplitude.

In terms of the steady perpendicular blowing amplitude, the lift and drag characteristics are found to become worst when the blowing amplitude increased beyond 0.1 (2.5×10^{-4} of the momentum coefficient). This is because the smaller amplitude of blowing can increase the momentum that helps in enhancing the mixing of fluid in the mainstream and the boundary layer region. Thus, reducing the drag, increasing the lift and the lift to drag ratio. While the higher amplitude of blowing will disturb and obstructing the flow and eventually lower the lift to drag ratio.

Acknowledgement

References

[1] Mohd Kamil, Muhammad Anas. *"Numerical Simulation of Airflow over Three Different Types of Airfoil."*. B.Eng. Thesis, Universiti Tun Hussein Onn Malaysia, 2017.

[2] Patel, Karna S., Saumil B. Patel, Utsav B. Patel, and Ankit P. Ahuja. "CFD Analysis of an Aerofoil." *International Journal of Engineering Research* 3, no. 3 (2014): 154-158.

[4] Mahmud, Md Shamim. "Analysis of Effectiveness of an Airfoil with Bi-camber Surface." *International journal of Engineering and Technology* 3, no. 5 (2013): 569-577.

[5] Jain, Shubham, Nekkanti Sitaram, and Sriram Krishnaswamy. "Computational investigations on the effects of Gurney flap on airfoil aerodynamics." *International scholarly research notices* 2015 (2015): 1-11.

[6] Siauw, W. L., and J. P. Bonnet. "Transient phenomena in separation control over a NACA 0015 airfoil." *International Journal of Heat and Fluid Flow* 67 (2017): 23-29.

[7] Shan, Hua, Li Jiang, and Chaoqun Liu. "Direct numerical simulation of flow separation around a NACA 0012 airfoil." *Computers & fluids* 34, no. 9 (2005): 1096-1114.

[8] James, Sandeep Eldho, Abhilash Suryan, Jiss J. Sebastian, Abhay Mohan, and Heuy Dong Kim. "Comparative study of boundary layer control around an ordinary airfoil and a high lift airfoil with secondary blowing." *Computers & Fluids* 164 (2018): 50-63.

[9] Lee, Sang, Eric Loth, and Holger Babinsky. "Normal shock boundary layer control with various vortex generator geometries." *Computers & Fluids* 49, no. 1 (2011): 233-246.

[10] Huang, L., P. G. Huang, R. P. LeBeau, and Th Hauser. "Numerical study of blowing and suction control mechanism on NACA0012 airfoil." *Journal of aircraft* 41, no. 5 (2004): 1005-1013.

[11] Prakash, Bhanu, Fernando Mellibovsky Elstein, and Josep Maria Bergadà Granyó. "Parametric analysis of active flow control using steady suction and steady blowing." In *Proceedings of the 17th International Conference on Computational and Mathematical Methods in Science and Engineering, CMMSE 2017, Costa Ballena (Rota), Cádiz, Spain, July 4-8, 2017*, pp. 1712-1721. 2017.

[12] Deng, Shutian, Li Jiang, and Chaoqun Liu. "DNS for flow separation control around an airfoil by pulsed jets." *Computers & Fluids* 36, no. 6 (2007): 1040-1060.

[13] De Giorgi, M. G., C. G. De Luca, A. Ficarella, and F. Marra. "Comparison between synthetic jets and continuous jets for active flow control: application on a NACA 0015 and a compressor stator cascade." *Aerospace Science and Technology* 43 (2015): 256-280.

[14] You, D., and P. Moin. "Active control of flow separation over an airfoil using synthetic jets." *Journal of Fluids and Structures* 24, no. 8 (2008): 1349-1357.

[15] Zhao, Guoqing, and Qijun Zhao. "Parametric analyses for synthetic jet control on separation and stall over rotor airfoil." *Chinese Journal of Aeronautics* 27, no. 5 (2014): 1051-1061.

[16] Lefebvre, A., B. Dano, W. B. Bartow, M. D. Fronzo, and GeCheng Zha. "Performance and energy expenditure of coflow jet airfoil with variation of mach number." *Journal of Aircraft* 53, no. 6 (2016): 1757-1767.

[17] Abinav, R., Nandu R. Nair, P. Sravan, Pradeesh Kumar, and S. R. Nagaraja. "CFD Analysis of Co Flow Jet Airfoil." *Indian Journal of Science and Technology* 9 (2016): 45.

[18] Yousefi, Kianoosh, S. Reza Saleh, and Peyman Zahedi. "Numerical study of flow separation control by tangential and perpendicular blowing on the NACA 0012 airfoil." *International Journal of Engineering* 7, no. 1 (2013): 10-24.

[19] Paisal, Muhammad Sufyan Amir. "Numerical Simulation of Flow Over Airfoil Using Open Source Algorithm." PhD diss., Universiti Tun Hussein Onn Malaysia, 2016.

[20] Hakim, Muhammad Syahmi Abdul, Mastura Ab Wahid, Norazila Othman, Shabudin Mat, Md Shuhaimi Mansor, Nizam Dahalan, and Wan Khairuddin Wan Ali. "The Effects of Reynolds Number on Flow Separation of Naca Aerofoil." *Journal of Advanced Research in Fluid Mechanics and Thermal Sciences* 47, no. 1 (2018): 56-68.